Preparation and Free Radical Detection of Doped ZnO Nanomaterials

Shanshan Song, Yuguang Lv*, Bo Wang, Qi Shi, Yaxin Zhao, Ziran Zhou
College of Pharmacy, Jiamusi University, Heilongjiang, Jiamusi 154007, China
E-mail: yuguanglv@163.com

Abstract: Nanomaterials play an important role in the field of optics and medicine, and rare earth cerium can act as a catalyst and a dopant to increase improve its optical properties. Used nanometer zinc oxide as a carrier, the Ag-ZnO and Ag-Ce-ZnO samples were prepared with the sol-gel method and characterized by X-ray diffractometer. The nanometer zinc oxide materials can generate the free hydroxyl radicals, so the methylene blue solution (MB) was used as the capture agent, and the free radicals produced by the doped nanometer zinc oxide were detected by UV-spectrophotometry. The results showed that the preparation particle size of the Ag-ZnO sample was about 75nm, particle size of the Ag-Ce-ZnO sample was about 70nm. The concentration of two samples treated with the dispersant PAAS generated hydroxyl radicals is much larger than the two samples treated with the dispersant SDBS. The doping of Ce ions not only improved the optical activity of the samples, but also increased the content of hydroxyl radicals. Rare-earth doped effe ctively improved the optical properties of the ZnO nanoparticles, and the effect of sample Ag-Ce-ZnO was better than Ag-ZnO samples. Discussion and study on the nature of both the nanometer zinc oxide and doped nanometer zinc oxide, as well as the method of preparation and the theory of produce hydroxyl radicals. In the experiment, doped nano-ZnO was used as carrier and methylene blue (MB) as capture reagent. This study provided a new method for the detection of free radicals drugs.
Keywords: spectrophotometry; nano-zinc oxide; sol-gel; methylene blue; free radicals.

1. Introduction

According to records, due to the unique physical and chemical activity of rare earth ions, has been greatly used to improve the characteristics of functional materials[1]. Therefore, doped with rare earth metal ions in recent years has become a hot research direction [2-3]. Because of rare earth cerium has good catalytic properties and optical properties, in the case of not introduce new material, rare earth cerium can act as a catalyst and a dopant to increase improve its optical properties [4-6]. In this paper, the introduction of the Ce^{4+} made particle size distribution of nanometer ZnO become, the ultraviolet absorption spectrum of nanometer ZnO was slightly blue-shifted, and it broadened compared with the absorption spectrum of nanostructured ZnO which not doped Ce^{4+} ions. However, the smaller the particle size of nanometer ZnO[7-8], the higher the surface activity of nanometer ZnO, then easy to lead to spontaneous formation of agglomeration, it was required to be dispersed with the surfactant[9].

Semiconductor electronic structure of ZnO is a kind of catalyst [10-12], under the irradiation of light, when a certain energy photons or over the semiconductor energy band gap (Eg) photons into the semiconductor, from the valence band VB inspire to the conduction band CB an electron, leaving a hole [13-15]. Excited states of the conduction band electrons and valence band holes can be eliminated by restructuring to input energy and heat, on the surface of the material capture electron, valence electron transition to the conduction band, hydroxyl electrons in the surrounding environment are made into free radicals[16-18]. Due to the short life of hydroxyl radicals (less than 10^{-4} s), and the small concentration, they can not be directly measured, so it is necessary to chase the hydroxyl radicals with capture agent, and then indirectly determined. Spectrophotometry [19], is also known as absorption spectroscopy, that is, at a particular wavelength or within a certain wavelength range, to determine the measured value or luminous intensity of the measured material, and then the material was analyzed quantitatively and qualitively. It is mainly used for the identification of drugs, inspection and determination of content [20].

2 Experimental

2.1 Instruments and materials

UV-vis spectrophotometer (UV-2550), digital pH meter (Germany sartorius), electronic balance (FA2004, Shanghai experiment instrument factory co., LTD.), constant temperature magnetic stirrer (85-1, Guangzhou China electrical appliance co., LTD.), the ultrasonic instrument (DS-2510 DTH, Shanghai), X-ray diffraction (3-IIIC, master company in Japan), vacuum drying oven (DZF-6020, Nanjing GengChen), pipe type resistance furnace (Zhuanghe South survey machinery factory).

Ethylene glycol, methyl ether, ethanolamine, two hydrated zinc acetate, silver nitrate and cerium nitrate, acetic acid glacial, methylene blue (AR), secondary distilled water, buffer solution (AR, pH = 7.0), SDBS (AR), PAAS (AR).

2.2 Methods

2.2.1 Preparation of sample (sol-gel)

1) The preparation of ZnO-Ag

80 ml glycol-methyl ether (as solvent) and 80 ml of ethanol amine (as a stabilizer) were mixed and heated to 60 °C in a water bath. The zinc nitrate dihydrate was added under vigorous stirring (the concentration of zinc ions in the solution was 0.3 M), the amount of silver nitrate added was 2% of the doping amount, 6 mL of glacial acetic acid (as a catalyst) was added. The mixture was stirred for 2 hours to obtain ZnO-Ag gel, ultrasonic for 1 hour, then placed at room temperature for 8h, took the supernatant, gel was dried in vacuum at 70 ℃ , and was sintered in vacuum at 450 ℃ to obtain nano-ZnO-Ag powder.

2) The preparation of Ag-ZnO-Ce

80 ml glycol-methyl ether (as solvent) and 80 ml of ethanol amine (as a stabilizer) were mixed and heated to 60 °C in a water bath. The zinc nitrate dihydrate was added under vigorous stirring (the concentration of zinc ions in the solution was 0.3 M), the amount of silver nitrate added was 2% of the doping amount, and the amount of cerium sulfate tetrahydrate added was 2% of the doping amount, 6 mL of glacial acetic acid (as a catalyst) was added. The mixture was stirred for 2 hours to obtain ZnO-Ag gel, ultrasonic for 1 hour, then placed at room temperature for 8h, took the supernatant, gel was dried in vacuum at 70 ℃ , and was sintered in vacuum at 450 ℃ to obtain nano-ZnO-Ag-Ce powder.

2.2.2 X-ray diffraction analysis of sample

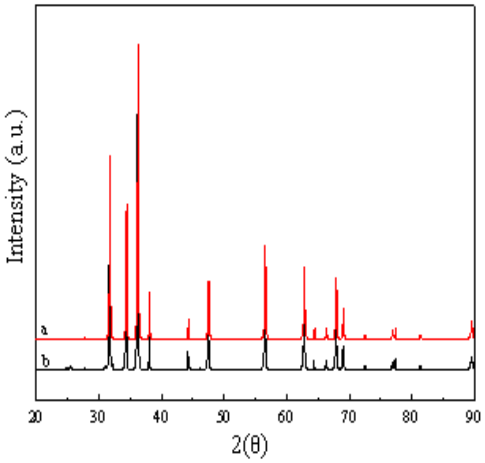

Fig. 1. XRD diffraction diagrams of the samples Ag-ZnO(*a*) and Ag-Ce-ZnO (*b*).

In this experiment, a sample solution of Ag-ZnO(*a*) and a sample solution of Ag-Ce-ZnO (*b*) were prepared, and X-ray diffraction analysis was carried out. Fig. 1 was the XRD pattern of the two samples in the 2θ range from 20 to 90°. A part of the diffraction peaks of Ce and Ag can be observed, indicating that a small amount of the dopant elements were present in the material in the form of a simple substance, and a part of the elements were dissolved in the ZnO lattice. The average particle size of the two Ag-Ce-ZnO samples calculated by the Scherrer formula were about 75 nm (*a*) and 70 nm (*b*), respectively. The results showed that the doping of rare earth elements can significantly inhibit the growth of nano-Ag-ZnO grains.

2.2.3 Scanning electronic microscope analysis of sample

Fig. 2 was an electron micrograph of the samples (*a*) and (*b*). The two samples obtained by the sol-gel method were slightly agglomerated. The average particle size of Ag-ZnO(*a*) was about 75 nm, and the average particle size of Ag-Ce-ZnO (*b*) was about 70 nm. The particle size of the sample was consistent with the predicted value of the Scherrer formula.

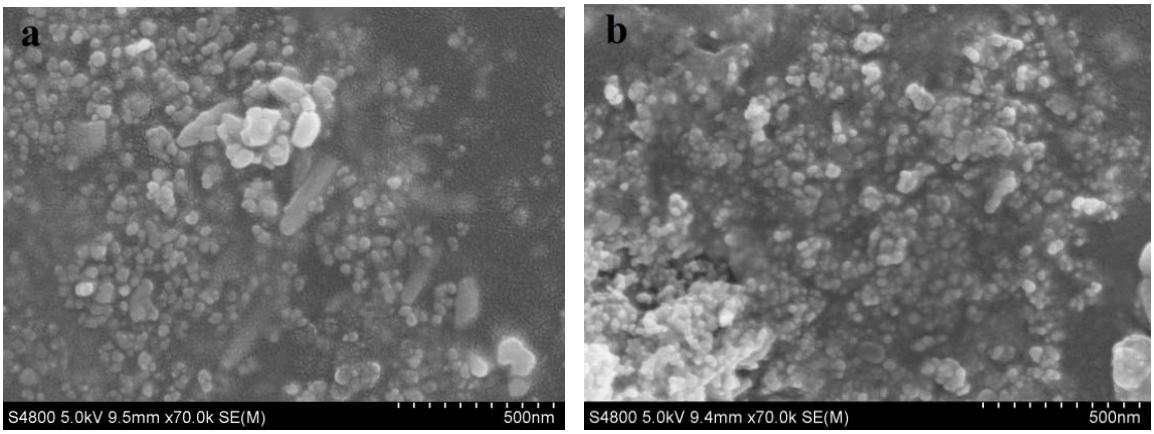

Fig. 2. Scanning electron microscopy (SEM) images of the samples (*a*) and (*b*).

2.2.4 Preparation of stock solution

1) Preparation of SDBS Dispersed Samples

0.21 g of Ag-ZnO and 0.21 g of Ag-Ce-ZnO were added with 250 mL of distilled water and 0.17 g of SDBS respectively. The pH of the mixed system was adjusted to 7.5 with an acidity meter and dispersed for 4 hours with an ultrasonic system. After standing for 4 days at room temperature, took 1 mL of the supernatant into a 100 mL volumetric flask as the stock solution. It was diluted to the different concentrations when used (select the six concentration gradient for a group).

2) Preparation of PAAS Dispersed Sample

0.21 g of Ag-ZnO and 0.21 g of Ag-Ce-ZnO were weighed into the agate mortar for 20 minutes, then 62.5 mL of PAAS aqueous solution was added and the grinding was continued for 10 minutes. The addition amount of PAAS was 25% and the pH of the mixed system was adjusted to 9.0 with an acidity meter, then fixed to 250 mL, stirred at room temperature in a magnetic stirrer for 15 minutes, dispersed for 30 minutes with an ultrasonic system. After standing for 4 days at room temperature, took 1 mL of the supernatant into a 100 mL volumetric flask as the stock solution. It was diluted to the different concentrations when used (select the six concentration gradient for a group).

2.3 Test methods

2 mL of the stock solution was added to the 10 mL colorimetric tube, and added 2 mL of methylene blue solution and 5 mL of the buffer solution, then mixed. After 5 minutes of reaction, the absorbance was measured at a wavelength of 664 nm with a 1 cm cuvette, and used water as a reference. Similarly, the absorbance of the corresponding blank methylene blue solution of the single ZnO sample is measured.

3. Results and Discussion

3.1 The influence of pH and buffers

The absorbance of the doped ZnO system was measured in the range of pH 3.0 to 9.0, and the results were shown in Fig. 3. As shown in the Fig. 3, the absorbance of the system was increasing at pH 2.0 to 7.0, and the absorbance was maximized at pH = 7.0. Therefore, pH = 7.0 was chosen for the optimum pH. The effects of the different buffer solutions (Tris-HCl buffer solution, NH_4Ac-HAc buffer solution, NaAc-HAc buffer solution, Na_2HPO_4-KH_2PO_4 buffer solution) on the absorbance of the system were tested under the condition of pH = 7. The experimental results showed that 0.01 $mol.L^{-1}$ Tris-HCl buffer solution is the best.

3.2 The effect of the concentration of the methylene blue solution

The methylene blue solution was scanned with an ultraviolet spectrophotometer and the maximum absorption at a wavelength of 664 nm. The experimental results showed that the concentration of methylene blue solution had a good linear relationship with the absorbance in the range of 20×10^{-6} $mol.L^{-1}$ to 140×10^{-6} $mol.L^{-1}$.

3.3 The effect of addition order of the reagent

The experimental results showed that the addition order of reagents can affect the system absorbance, and the best experimental effect was added the sample solution firstly, then added methylene blue and buffer. After 5 minutes the doped ZnO system can produce hydroxyl radicals at room temperature.

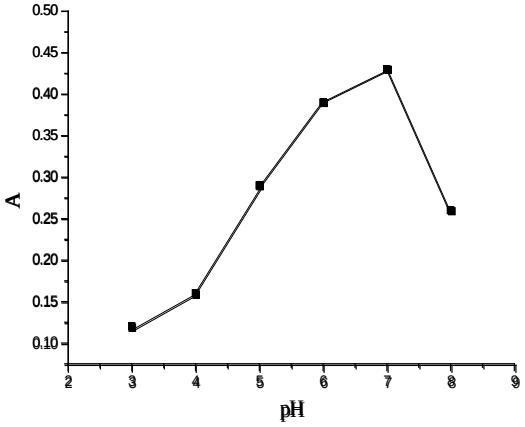

Fig. 3. Effect of pH on the absorbance of the system.

3.4 The analysis of the two samples dispersed with SDBS

3.4.1 The analysis of Ag-ZnO sample

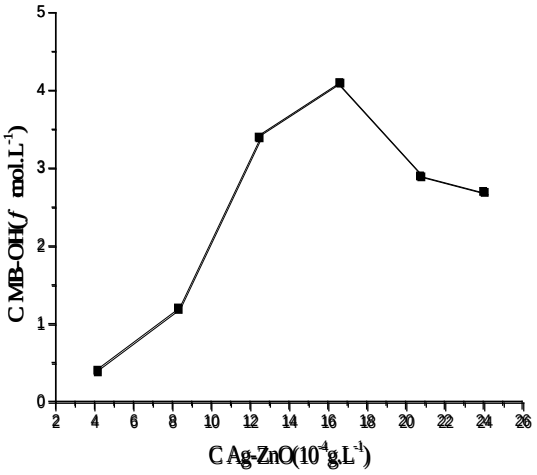

Fig. 4. The relationship between concentrations of samples of MB-OH and Ag-ZnO.

As shown in Fig. 4, the concentration of MB-OH increased first then decreased, and finally had no significant change with the increase of the concentration of Ag-ZnO sample (the concentration of MB was 60 μmol.L^{-1}, and the concentration of SDBS was 20 μmol.L^{-1}).

3.4.2 The analysis of Ag-Ce-ZnO sample

As shown in Fig. 5, the concentration of MB-OH increased first then decreased rapidly with the increase of the concentration of Ag-Ce-ZnO sample (the concentration of MB was 60 μmol.L^{-1}, and the concentration of SDBS was 20 μmol.L^{-1}).

3.5 The analysis of the two samples dispersed with PAAS

3.5.1 The analysis of Ag-ZnO sample

The concentration of MB-OH was high when the concentration of Ag-ZnO was low in Fig. 6. With the increase of the concentration of Ag-ZnO, the concentration of MB-OH increased first to reach the peak quickly, then decreased to a certain value, and finally increased slowly (the concentration of MB was 60 μmol.L^{-1}, and the concentration of PAAS was 20 μmol.L^{-1}).

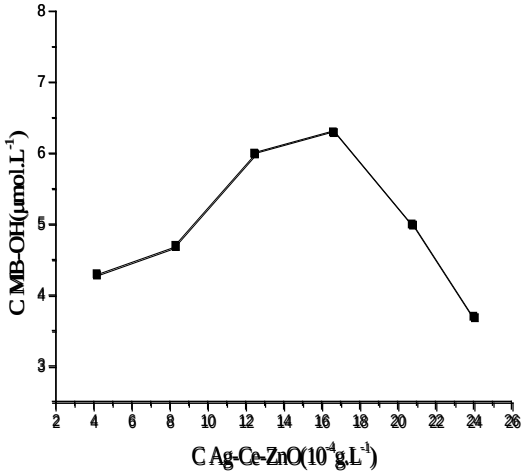

Fig. 5. The relationship between concentration of MB-OH and the concentration of Ag-Ce-ZnO.

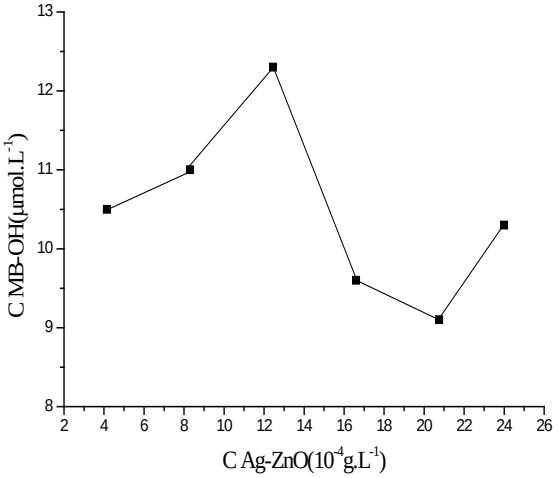

Fig.6. Relationship between concentration of MB-OH and Ag-ZnO concentration.

3.5.2 The analysis of Ag-Ce-ZnO sample

As shown in Fig. 7, when the Ag-Ce-ZnO sample concentration was low, the concentration of MB-OH reached the peak quickly. With the increase of the concentration of Ag-Ce-ZnO sample, the concentration of MB-OH decreased slowly, and then slowly increased (the concentration of MB was 60 μmol.L^{-1}, and the concentration of PAAS was 20 μmol.L^{-1}).

3.6 The analysis of four samples dispersed with two kinds of dispersants

As shown in Fig. 8, the concentrations of the hydroxyl radicals produced by the same sample were different after the Ag-ZnO sample and the Ag-Ce-ZnO sample were treated with two different dispersants. The concentration of hydroxyl radicals produced by the two samples treated with the PAAS dispersant was much greater than that of the two samples treated with the SDBS dispersant. Ag-Ce-ZnO samples had stronger ability to produce hydroxyl radicals than Ag-Ce-ZnO samples, and the rare earth Ce ions can significantly increase the activity of Ag-ZnO. When the Ag-Ce-ZnO sample concentration was low, the concentration of MB-OH can reach the peak, and the sample doped with Ce ions had the minimum effective concentration when the sample concentration was similar. It was showed that the doping of Ce ions not only improved the optical activity of the sample, but also improved the free radical content of the sample(the concentration of MB was 60 μmol.L^{-1}, the concentration of PAAS was 20 μmol.L^{-1} and the concentration of SDBS was 20 μmol.L^{-1}).

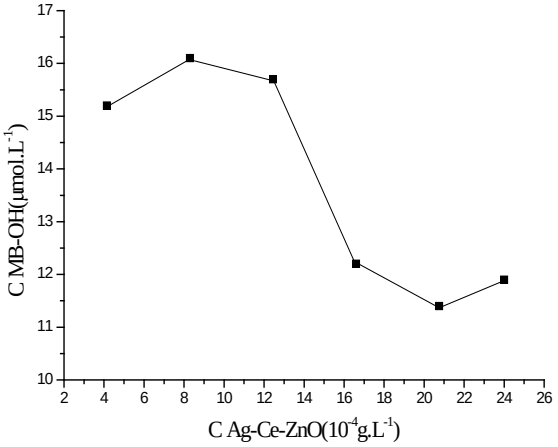

Fig.7. Relationship between concentration of MB-OH and the concentration of Ag-Ce-ZnO.

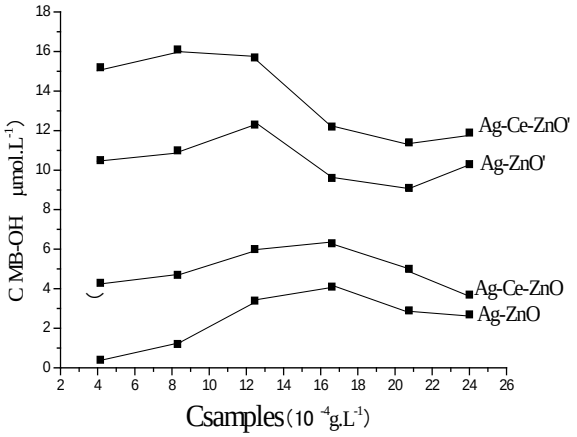

Fig. 8. The relationship between the concentration of four samples and the concentration of MB-OH.

3.7 Calculation

The relationship between the concentration of MB solution and the absorbance value of the system (wavelength at 664 nm) was shown in Fig. 9. (The concentration of MB-OH solution were 20×10^{-6} mol.L^{-1},30×10^{-6} mol. L^{-1}, 40×10^{-6} mol.L^{-1},50×10^{-6} mol.L^{-1},60×10^{-6} mol.L^{-1},70×10^{-6} mol.L^{-1}) According to Fig. 9, the standard curve equation of the concentration of MB and the absorbance value can be obtained:

$$A=0.0159C_{MB}+0.057 \quad (1)$$

From formula: $C_{MB}= (A+0.057)/ 0.0159$ (2)

We can know that : $C_{\cdot OH}=C_{MB1}- C_{MB2}= (A_1 - A_2) / 0.0159$ (3)

(Annotations: $C_{\bullet OH}= C_{MB\text{-}OH}$)

4. Conclusions

The experimental results showed that the method of detecting the hydroxyl radical in the sample with ultraviolet spectrophotometer used methylene blue as the capture agent had the advantages of simplicity, high sensitivity, low price and good stability. This method provided a simple means for the detection of free radicals.

Acknowledgments

This work was project supported by National Science Foundation of China(No. 21346006), Department of scientific research project in Heilongjiang province (No. B2017015), Scientific research project of Heilongjiang province education department (No.12541783), National project training project of Jiamusi University (No.JMSUJCGP 2016-003), Support was also given by the Key Laboratory of Photochemistry, Institute of

Chemistry, Chinese Academy of Sciences, and the Key Laboratory of Luminescence and Optical Information, Beijing Jiaotong University.

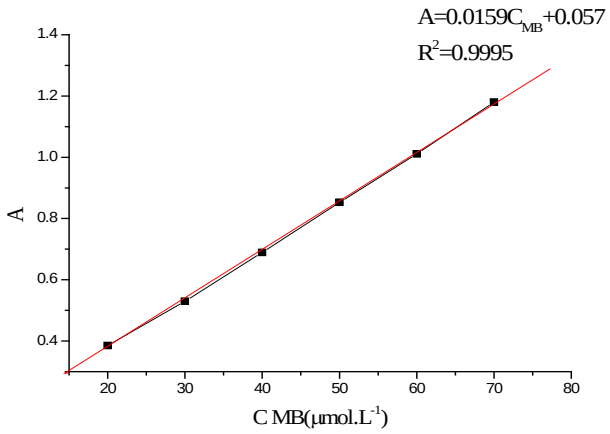

Fig. 9. The linear relationship between the concentration and absorbance of MB.

5. References

[1] Chen, H.L., Wang, S.L., Bao, B.S. Preparation and Electrical Properties of Nanocomposites. Functional Materials, 2014, 45(7): 7035-7038.

[2] Wang, H.H., Chen, Y.S., Zhou, J.P. Hydrothermal Preparation and Rare Earth Doping of Zinc Oxide. Journal of Synathetic Crystals, 2012, 41(5): 1250-1253.

[3] Cao, Y., Wang, Y.T., Xu, Y.Q. Preparation of Rare Earth Ions Doped ZnO Nanoparticles by Microwave Induced Combustion. Bulletin of the Chinese Ceramic Society, 2012, 31(5): 1317-1321.

[4] Rahul, K.S., Anja, V.M., Pushpal, G. Recent trends in binary and ternary rare-earth fluoride nanophosphors: How structural and physical properties influence optical behavior. Journal of Luminescence, 2017, 189: 44-63.

[5] Yin, Q.Q., Qiao, R., Tong, G.X. Preparation and Application of Ion-Doped ZnO Oxide Photocatalytic Nano Functional Materials. Progress in Chemistry, 2014, 26(10): 1619-1632.

[6] Kang, J.L., Yao, L.F., Yang, S.L. Preparation and Photocatalytic Activity of Ce-doped TiO_2 Nanocomposite Films. Journal of Synthetic Crystals, 2013, 42(4): 671-676.

[7] Ali, R.R., Saeid, J.M., Reza, M.S., Majid, G. Barium Doped ZnO Nano-Particles: Preparation and Evaluation of their Catalytic Activity. Current Nanoscience, 2014, 10: 312-317.

[8] Shi, L., Xu, Y.M., Li, Q. Preparation and Growth Mechanism of ZnO Nanotubes ArrayJournal. Current Nanoscience, 2009, 5(3): 262-265.

[9] Chen, J.Y., Li, N., Fang, J.F. Effect of Surfactant on Dispersion and Sedimentation of Nanoparticles in Water. Journal of ZheJiang University of Technology, 2012, 40(6): 595-598.

[10] Ceng, G., Zhou, X.D., Li, Y. La^{3+} Modification and Photocatalytic Activity of Nano-ZnO-TiO_2 Composite Semiconductor. Chinese Journal of Catalysis, 2007, 28(10): 885-889.

[11] Guo, X.G., Ma, J.Q., Ge, H.G. Preparation and Characterization of Nano - ZnO / Ag Containing Core - shell Structure and Its Photocatalytic Activity. Journal of Synthetic Crystals, 2014, 43(4): 967-971.

[12] Zu, Y., Qu, W.W., Peng,J.H. Research Progress of Photocatalysis of ZnO Carbon - based Composites. New Chemical Materials, 2014, 42(8): 205-207.

[13] Chai, L.Y., Liu, S.Y., Yang, Y. Preparation of ZrO_2 and Zinc Oxide Composites and Study on NOX Gas Sensitivity at Room Temperature. Journal of Synthetic Crystals, 2013, 42(8): 1611-1613.

[14] Chen, Z., Zhu, L., Wang, X. Preparation and Photocatalytic Activity of Zinc Oxide Nanomaterials. Chinese Journal of Environmental Engineering, 2016, 10(8): 4105-4108.

[15] Zhai, H.J., Jiang, S., Cheng, X. Preparation of ZnO - based Composites and New Progress in Photocatalytic Application. New Chemical Materials, 2016, 44(9): 13-14.

[16] Li, G.T., Song, H.Y., Liu, B.T. Generation and Effectiveness of Hydroxyl Radical in Photocatalytic Process. Chinese Journal of Enviromental Engineering, 2012, 6(10): 3388-3391.

[17] Zhang, H., Ren, F.Z. Advances in the Detection of Hydroxyl and Superoxide Free Radicals. Spectroscopy and Spectral Analysis, 2009, 29(4): 1093-1097.

[18] Wang, Z.F. Evaluation of Fruit Antioxidant Capacity by Free Radical Method. *Spectroscopy Laboratory*, 2013, 30(1): 151- 153.
[19] Tian, T., Zhu, J.J., He, Y. A New Hydroxyl Radical Generation Method and Its Application in Methylene Blue Degradation. Journal of Hubei University, 2014, 36(5): 448-450.
[20] Zhang, D., Xu, B., Zhu, P. Study on Photocatalytic Degradation of Methylene Blue by TiO_2. Journal of East China Normal University, 2013, 5: 35-42.